ELSEVIER

Carbohydrate Polymers 47 (2002) 377–385

Carbohydrate Polymers

www.elsevier.com/locate/carbpol

Spectrophotometric detection of methyl cellulose–manganate(VI) intermediate complex in the oxidation of methyl cellulose by alkaline permanganate

Rafat M. El-Khatib*

Department of Chemistry, Faculty of Science, South Valley University, Sohag, Egypt

Received 23 October 2000; revised 8 December 2000; accepted 22 February 2001

Abstract

The formation of (methyl cellulose (MC)–$\mathrm{Mn^{(VI)}O_4^{2-}}$)

$$\mathrm{MC^-} + \mathrm{MnO_4^-} \overset{K_3}{\leftrightarrow} C_2 \xrightarrow{k_b} \left[\mathrm{MC{-}Mn^{(VI)}O_4^{2-}}\right]$$

where C_2 is a metastable state that interconverts into the [MC–$\mathrm{Mn^{(VI)}O_4^-}$] ester intermediate, during the oxidation of methyl cellulose polysaccharide at pH ≥ 12, was followed kinetically by spectrophotometric methods. The reaction was found to be first-order kinetics in [$\mathrm{MnO_4^-}$] and a fractional order in [MC]. Kinetic and spectrophotometric data confirmed the base-catalysed formation of Mn(VI) intermediate complex. A mechanism in agreement with the experimental data was assumed and discussed. © 2002 Elsevier Science Ltd. All rights reserved.

Keywords: Methyl cellulose; Oxidation; Mechanism; Intermediate; Rate; Permanganate

1. Introduction

The oxidation of organic compounds by permanganate has been extensively studied, in particular in acidic media (Hassan, Mousa & Wahdan, 1988b; Kumar & Sakena, 1970; Rao, Rajanna & Saiprakash, 1982; Rao, Sethuram & Rao, 1979; Verma, Reddy & Shastry, 1976). In a survey (Hassan, 1993a), not enough mechanistic information was available for the oxidation of macromolecules containing secondary alcoholic OH groups by this oxidant; this may be attributed to the complexity of the overoxidation. Therefore, in this work it is intended to undertake a further, extensive kinetic study of the alkaline oxidation of methyl cellulose (MC) at (pH ≥ 12) by permanganate, with the aim of discovering more details about the transition state. Under the present conditions, the oxidation proceeds via methyl cellulose manganate(VI) to form, finally, ketomethyl cellulose and $\mathrm{MnO_2}$. The latter inorganic reduction product can be filtered off after ageing and coagulation through a fine glass filter (Makhlouf, El-Shatoury & Hassan, 1992).

The importance of this oxidation is to get the green [Mn(VI–MC] and/or blue [Mn(V)–MC] intermediate species which were detected elsewhere (Hassan, 1993b; Hassan, Abd-Alla & El-Zohry, 1993; Jacky & Simandy, 1972, 1976a,b; Makhlouf et al., 1992; Wiberg, Deutsch & Rocek, 1973). Thus, the metastable (V) and (VI) valencies of Mn are detected for over a wide range (110–240 min) and its formation is followed and measured by conventional spectrophotometric methods. Moreover and finally, Monoketo and/or a diketobiopolymer of industrial importance is obtained (Hassan, 1993a,b; Hassan et al., 1988b; Makhlouf et al., 1992) Methyl cellulose is very important in the textile, oil detergent, and adhesive industries (abstracted from www.google.com website).

2. Experimental

The methyl cellulose used in this paper is one of the Sigma Chemical products (average molecular weight 50,000) calculated from the value of viscosity of 2% solution of MC = 4000 centipoise at 20°C. To characterize MC and its oxidation product, IR spectra were recorded (cf. Fig. 1); the decay and appearance of the band at 3450 and

---

* Fax: +20-093-601159.
E-mail address: shaker-ali@mailcity.com (R.M. El-Khatib).

0144-8617/02/$ - see front matter
PII: S0144-8617(01)00192-8

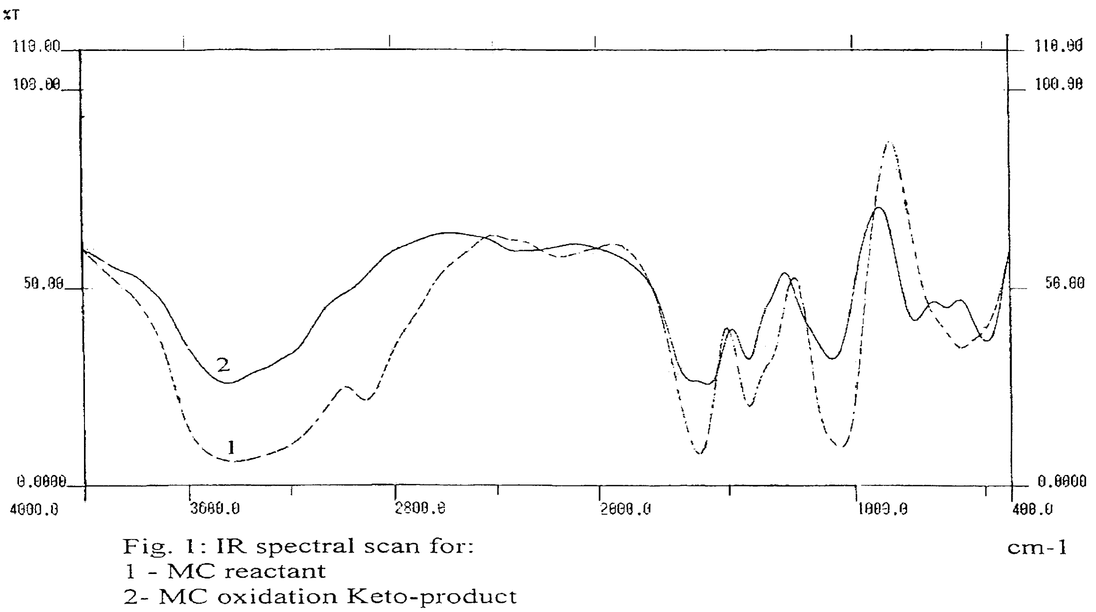

Fig. 1. IR spectral scans for: (1) the dotted line for MC-reactant; (2) the solid line for MC keto-oxidation product.

1700 cm^{-1}, respectively, indicates the interconversion of secondary OH^- to a (C=O) group.

Stock solutions of MC, sodium hydroxide, perchlorate, and potassium permanganate were prepared by dissolving the calculated amounts of BDH AnalaR samples in redistilled water. The stock solution of $KMnO_4$ was standardized against As_2O_3, after which the permanganate ion concentration was determined spectrophotometrically, immediately prior to each run at 525 nm, the absorption maximum of permanganate (Hassan et al., 1988b). The stock permanganate was diluted to a suitable concentration before mixing with appropriate amounts of $HClO_4$ and $NaClO_4$ solutions.

3. Kinetic measurements

The kinetic measurements were performed so that the reaction follows pseudo-first-order rate law in $[MnO_4^-]$, where NaOH and MC exist in greater abundance than MnO_4^-. Total ionic strength was kept unvaried at

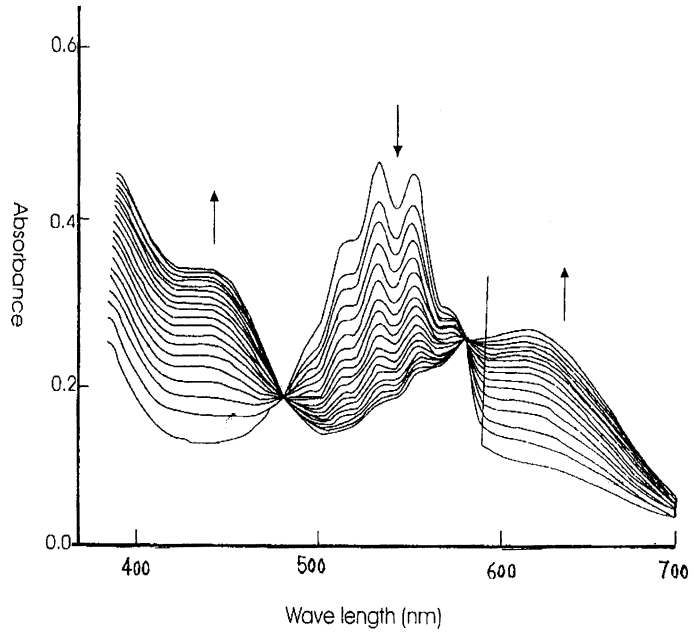

Fig. 2. Spectral trace (380–700 nm) for MC oxidation by alkaline permanganate; $[MC] = 4 \times 10^{-3}$, $[MnO_4^-] = 2 \times 10^{-4}$, $[OH^-] = 0.02$, $I = 0.1$ mol dm^{-3} at 20°C.

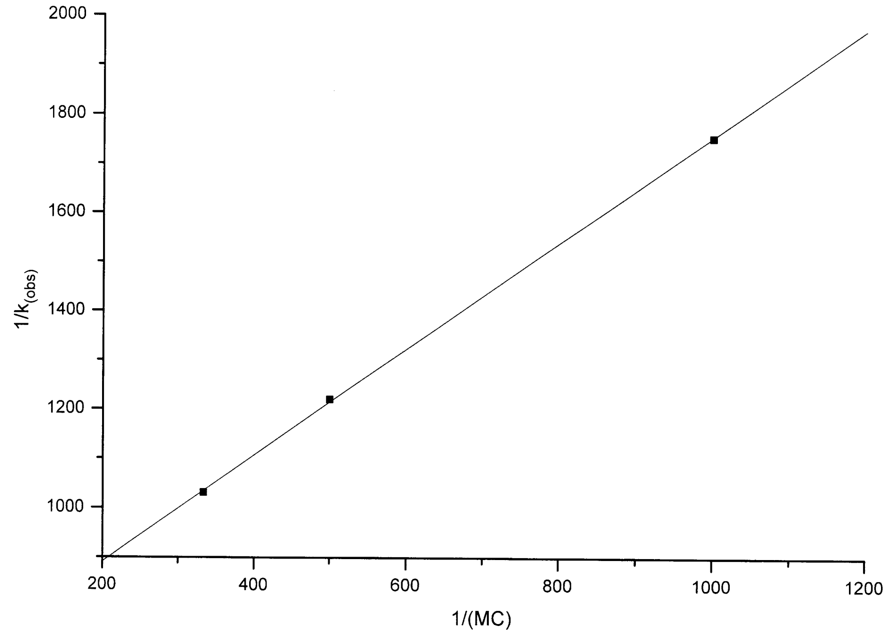

Fig. 3. $k_{\mathrm{obs.}}^{-1}$ against $[\mathrm{MC}]^{-1}$ plot for MC alkaline permanganate oxidation via the formation of the intermediate $[\mathrm{MC{-}Mn^{(VI)}O_4^{2-}}]$ at, $[\mathrm{MnO_4^-}] = 2 \times 10^{-4}$, $[\mathrm{OH^-}] = 0.04$, $I = 0.1$ mol dm^{-3}, at 20°C.

0.1 mol dm^{-3} with inert $NaClO_4$. The reaction solutions were thermally constant at 20 ± 0.1°C in a Haake F_3 ultrathermostat, then the required volumes were syringed out and poured into the reaction cell adjusted at the same ambient temperature by the thermostated water flow into the surrounding reaction cell jacket. The reaction was followed by recording the increase of absorbance at 610 nm, the absorption maximum of the green $[\mathrm{MC{-}Mn^{(VI)}O_4^{2-}}]$ intermediate complex as a function of time up to an almost constant value. Electronic spectra and absorbance values were recorded using a Cecil CE 599 automatic scanning spectrophotometer connected to a CE 836 cell and wavelength programmer. It was assumed that there was no interference from any other reagents at this wavelength; cf. Fig. 2.

It is worth mentioning that the absorbance A_∞ at $t = \infty$ at 610 nm as a function of $[\text{complex}] = \alpha[\mathrm{MnO_4^-}]_0$, where α is a proportionality constant, obeys Beer–Lambert's relation. This provides a spectrophotometric method for the determination of MC polysaccharide.

4. Results

4.1. Stoichiometry and product analysis

Different ratios of MC and permanganate were mixed at 0.04 and 0.1 mol dm^{-3} sodium hydroxide and constant ionic strength, respectively, then equilibrated for 48 h at room temperature. Estimation of the unreacted MnO_4 was made as described elsewhere (Hassan et al., 1988b). The stoichiometric ratio, $[\mathrm{MC}]_0/[\mathrm{MnO_4^-}]$ reacted, was found to be two.

The stoichiometric reaction can be represented by the following:

$$2(\mathrm{C_7H_{12}O_5})_n + 4\mathrm{MnO_4^-} = 2(\mathrm{C_7H_8O_5})_n + 4\mathrm{MnO_2} + 4\mathrm{OH^-} + 2\mathrm{H_2O} + \mathrm{O_2}$$

where $(\mathrm{C_7H_{12}O_5})_n$ is the methyl cellulose polymer (MC), and $(\mathrm{C_7H_8O_5})_n$ is the diketomethyl cellulose polymer of the structure of MC, the oxidation product. The diketo biopolymer would be represented (Hassan et al., 1993) as:

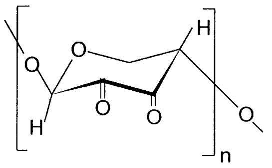

The yellow color which persists even after the completion of the oxidation reaction, then finally dispersed brown MnO_2 sol, may confirm that hypomanganate(V) formed and decomposed to Mn(IV) sol, then the latter coagulated by ageing to a MnO_2 precipitate. The latter can be isolated by the addition of excess NaF to the reaction mixture during stirring. The latter was stirred thoroughly at room temperature for 24 h and then formed MnF_4 filtered off. To isolate the diketo-biopolymer derivative a portion of the concentrated filterate from MnF_4 was acidified with dilute acetic acid at pH ≈ 6, then the acid of diketo-methyl cellulose polymer was precipitated by ethanol. The solid product was filtered off, washed several times with ethanol, dried under vacuum (Hassan et al., 1993), and then subjected to

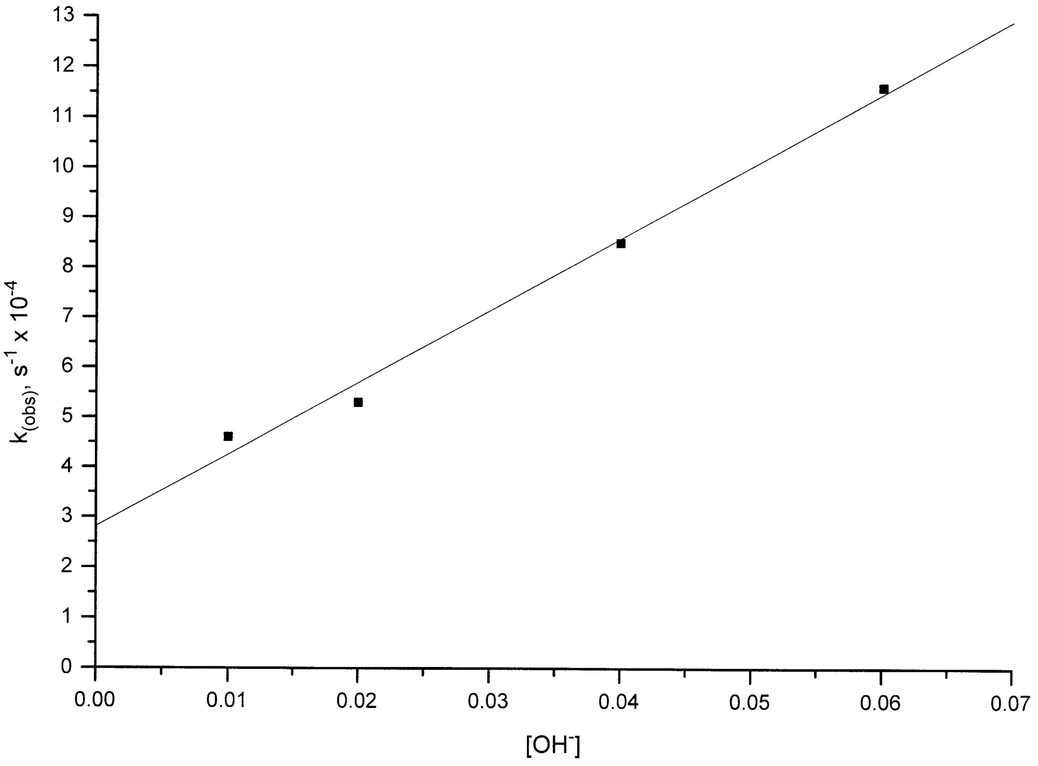

Fig. 4. $k_{obs.}$ versus [OH^-] linear plot in the formation of the intermediate complex during the oxidation of MC polysaccharide by alkaline permanganate, in the presence of [MC] = 4×10^{-3}, [MnO_4^-] = 2×10^{-4}, $I = 0.1$ mol dm^{-3}, at 20°C.

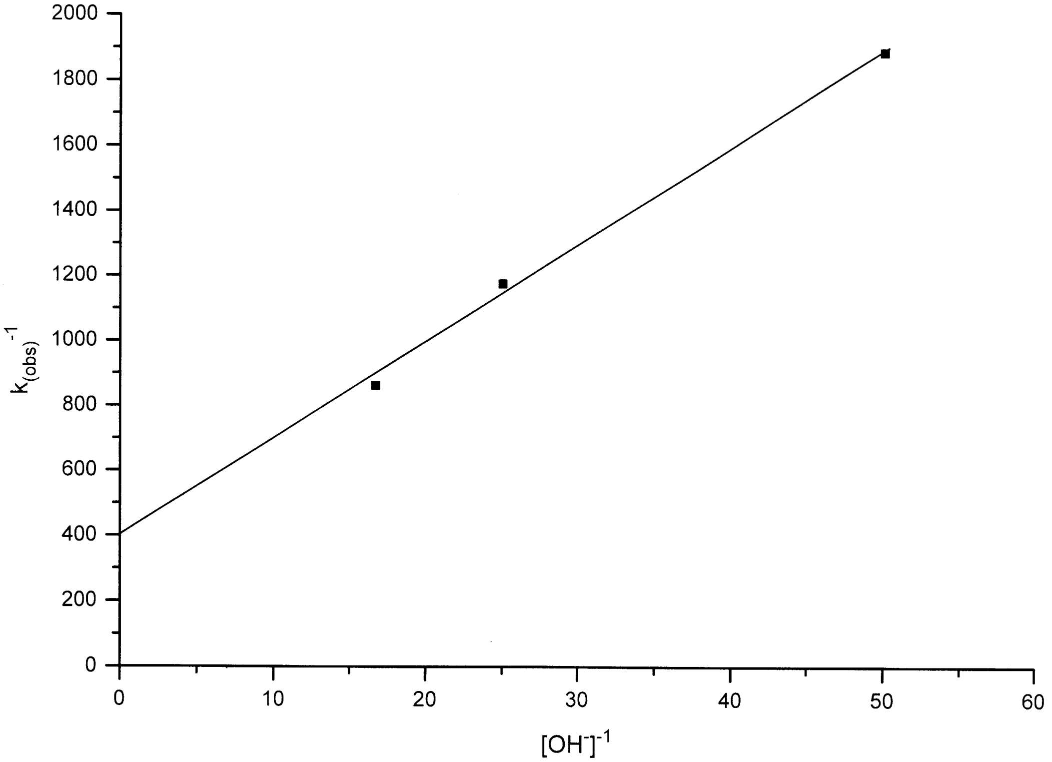

Fig. 5. $k_{obs.}^{-1}$–[OH^-]$^{-1}$ linear plot with a positive intercept for the oxidation of MC, at [MnO_4^-] = 2×10^{-4}, [MC] = 4×10^{-3}, $I = 0.1$ mol dm^{-3}, at 20°C.

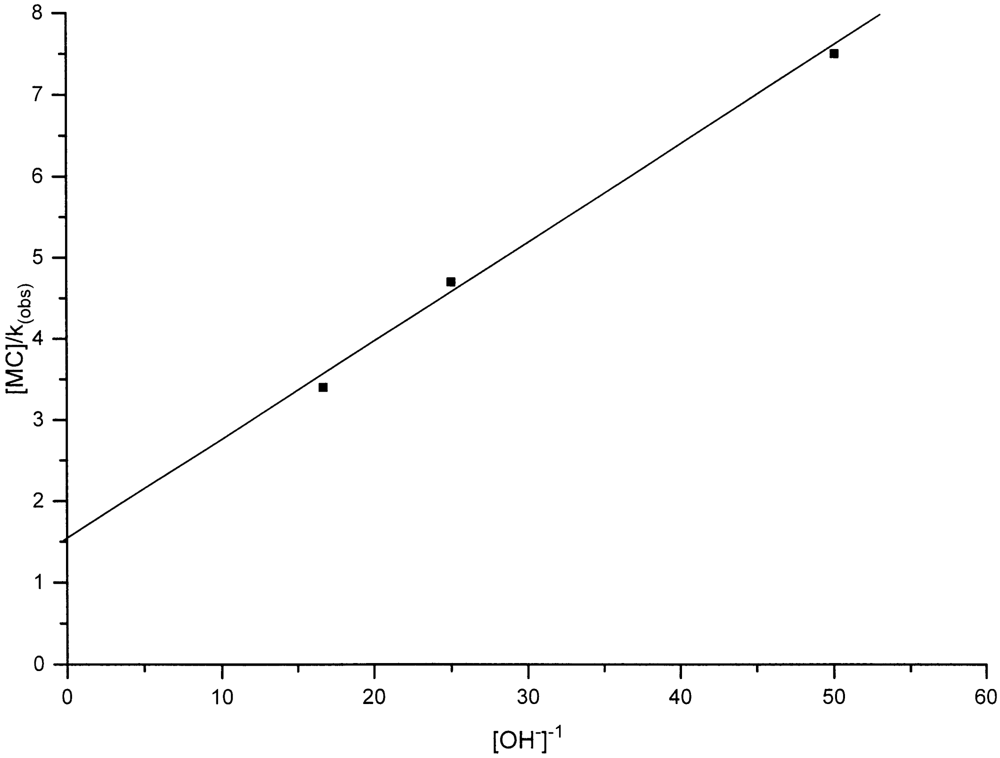

Fig. 6. $[MC]/k_{obs.}$–$[OH^-]^{-1}$ linear plot under the same conditions as Figs. 3 and 4.

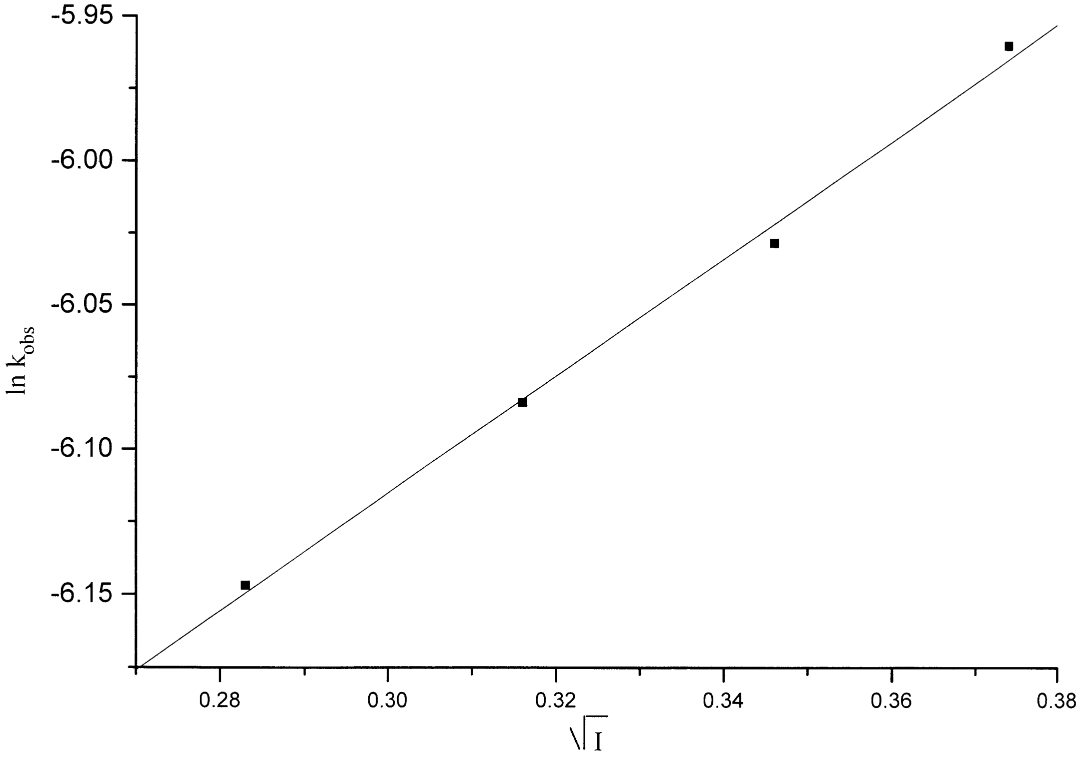

Fig. 7. ln $k_{obs.}$ against $\sqrt{I}$ for the formation of the intermediate complex $(MC–Mn^{(VI)}O_4^{2-}]$ in the oxidation of MC by the alkaline permanganate, at $[MC] = 4 \times 10^{-3}$, $[MnO_4^-] = 2 \times 10^{-4}$, $[OH^-] = 0.02$ mol dm^{-3}, at 20°C.

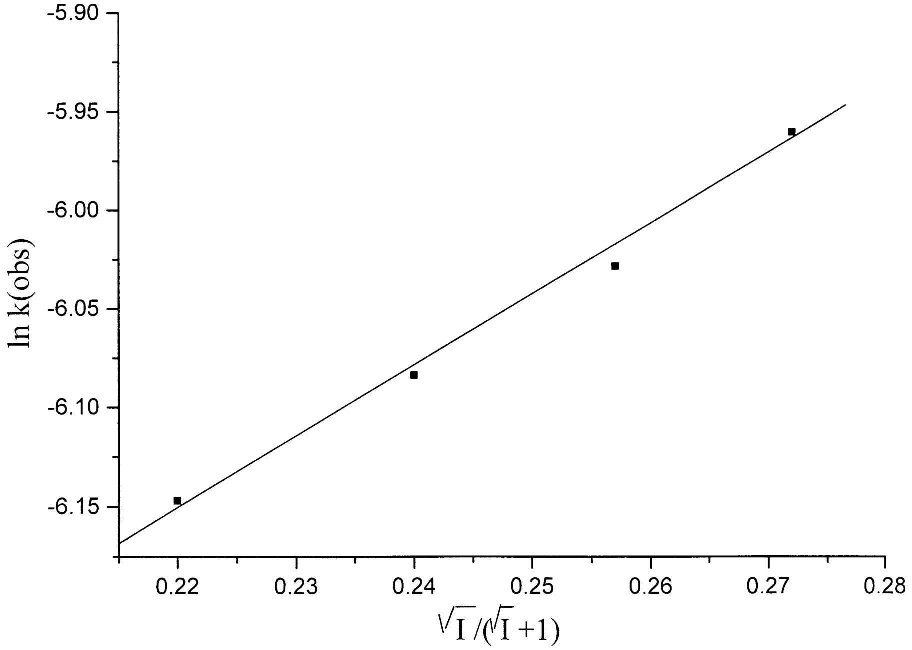

Fig. 8. ln $k_{\text{obs.}}$–$\sqrt{I}/(\sqrt{I}+1)$ linear plot with positive intercept for the alkaline oxidation of MC by permanganate through the formation of the intermediate $(\text{MC–Mn}^{(\text{VI})}\text{O}_4^{2-}]$ complex under the same conditions as Fig. 6.

IR spectroscopy and a red dinitrophenylhydrazone test. The melting point of the diketo derivative was found to be >300°C.

4.2. Polymerization test

The possibility of formation of free radicals was checked by treatment of the partially oxidized reaction mixtures with acrylonitrile. No polymerization formed, so the reaction does not proceed via a free radical mechanism as has been indicated previously (Hassan, 1993a,b).

4.2.1. Dependence of the reaction rate on $[\text{MnO}_4^-]$ and [MC]

It was found that the alkaline permanganate oxidation of MC followed first-order kinetics in $[\text{MnO}_4^-]$, i.e.

$$v = \frac{-\text{d}[\text{MnO}_4^-]}{\text{d}t} = k_{\text{obs.}}[\text{MnO}_4^-]$$

This result was indicated by the independent first-order rate constant values, given by least squares of the slopes of ln (absorbance) at 610 nm against time, on the initial concentration of MnO_4^-. But the first-order dependency in [MC] was not maintained due to intermediate formation (cf. Fig. 3).

The molar absorptivity of the intermediate complex was set out and found as $1.3 \times 10^3 \pm 50$ at $[\text{MnO}_4^-] = 2 \times 10^{-4}$, $[\text{MC}] = 4 \times 10^{-3}$, $[\text{OH}^-] = 0.02$, ionic strength $(I) = 0.1$ mol dm^{-3} at 20°C, and within the previously reported values (Hassan, 1993a,b; Hassan et al., 1988b).

4.2.2. Dependence of rate on $[\text{OH}^-]$

Experimental results indicated the base catalysed rate. Good linear $k_{\text{obs.}}$ versus $[\text{OH}^-]$ plots, at constant I, were obtained (cf. Figs. 4–6).

4.2.3. Effect of ionic strength on the reaction rate

With the aim of discovering more about the nature of the transition state, kinetic runs were arranged with different [salt] (NaClO_4) at $[\text{OH}^-] = 0.04$ mol dm^{-3}. The rate was

Table 1
Second-order rate constant values at various temperatures, activation parameters, Arrhenius factor for the formation of $[\text{MC–Mn}^{(\text{VI})}\text{O}_{4]}^{2-}$ intermediate complex at $\text{MnO}_4^- = 2 \times 10^{-4}$ $[\text{MC}] = 4 \times 10^{-3}$, $[\text{OH}^-] = 0.02$, $I = 0.1$ mol dm^{-3}, at 20°C (maximum error is 2% in activation parameters and 1% in rate constant values)

k_2[a] (dm^3 mol s^{-1})				E_a (kJ M^{-1})	$\Delta H^\#$ (kJ M^{-1})	$\Delta G^\#$ (J M^{-1} K^{-1})	$\Delta S^\#$ (kJ M^{-1})	A (M^{-1} s^{-1})
10°C	20°C	30°C	40°C					
0.255	–	0.345	0.428	14.90	9.93	75.97	− 220.4	135.5

[a] $k_2 = k_{\text{obs.}}/[\text{MC}]_\text{T}$ (cf. Eq. (7)).

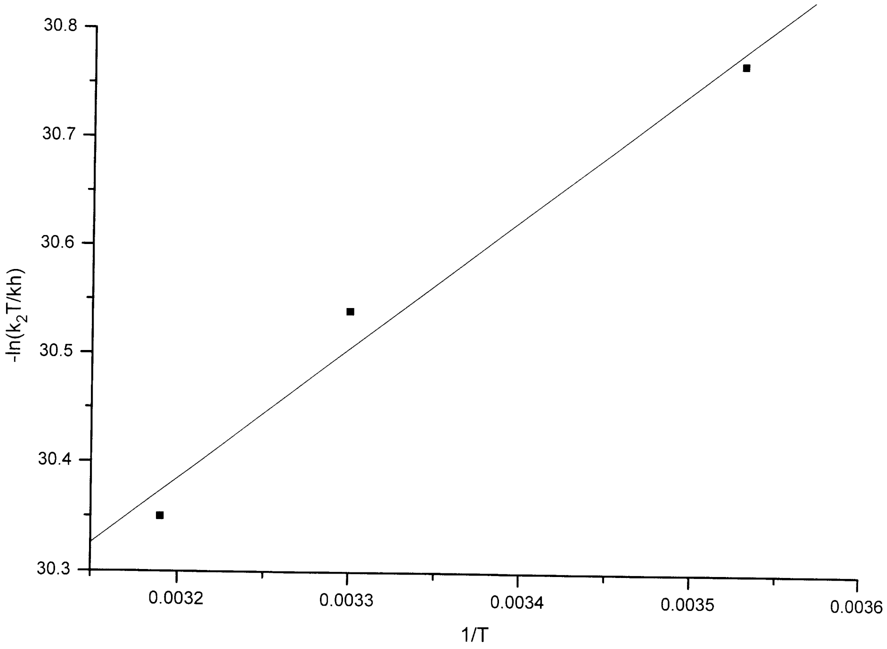

Fig. 9. Eyring plot ($-\ln(k_2h/kT)$ against ($1/T$) for the oxidation of MC by alkaline permanganate, at $[\mathrm{MC}] = 410^{-3}$, $[\mathrm{OH}^-] = 0.02$, $[\mathrm{MnO}_4^-] = 2\times10^{-4}$, $\mathrm{I} = 0.1\ \mathrm{mol\ dm}^{-3}$.

enhanced by added salts. Good linear plots of Bronsted–Bjerrum ($\ln k_{\mathrm{obs.}} - \sqrt{I}/(1+\sqrt{I})$ plot with positive intercept were obtained (cf. Figs. 7 and 8).

4.2.4. Activation parameters of the intermediate formation

The rate of reaction was speeded up by increasing the temperature. Moreover, the activation parameters were evaluated by least squares of Eyring and Arrhenius plots and then interpreted (Table 1 and Fig. 9).

5. Discussion

The repeat spectral scans in Fig. 2 indicate the interconversion of MnO_4^-, at absorption maximum ($\lambda_{\max} = 525$ nm), into both manganate(VI) intermediate complex of MC, at $\lambda_{\max} = 610$ nm, and MnO_2, at $\lambda_{\max} = 440$ nm (Hassan, 1993a,b; Hassan et al., 1988b; Makhlouf et al., 1992; Wei & Stewart, 1966). The isobestic points centered at 575 and 480 nm, respectively, demonstrated these interchanges. Many previous reports (Carrington & Symons, 1956; Jacky & Simandy, 1972, 1976a,b; Wei & Stewart, 1966; Wiberg & Geer, 1966; Wieberg et al., 1973) confirmed the formation of Mn(V) by stopped-flow techniques. But the short lifetime of hypomanganate(V) may be the reason why it has failed to be observed spectrophotometrically. The molar extinction coefficient, $\epsilon_{\max}$, of the MC-manganate(VI) complex was found to be $1.3\times10^3 \pm 50$ at $[\mathrm{MC}] = 4\times10^{-3}$, $[\mathrm{MnO}_4^-] = 2\times10^{-4}$, $[\mathrm{OH}^-] = 0.02$ and $I = 0.1\ \mathrm{mol\ dm}^{-3}$ at 20°C. This value is of the order of magnitude stated elsewhere for the corresponding intermediates with Alginate, poly(vinylalcohol) (Hassan, 1993a,b; Hassan et al., 1988b). The color reaction obeys Beer–Lambert's law, which would provide a useful colorimetric method for the determination of polysaccharides.

The experimental observation that the color reaction, after just mixing the reactants, changes from purple to blue and finally to green indicates the spectroscopically observable green intermediate complex and/or unstable hypomanganate(V) blue intermediate.

Again the naked eye observation and the linear $k_{\mathrm{obs.}}^{-1}$ versus $[\mathrm{MC}]^{-1}$ (Michaelis–Menten plot] obtained (Wei & Stewart, 1966), cf. Fig. 3, would support the oxidation of MC via the formation of the intermediate green manganate(VI) complex. Moreover, the good linear $k_{\mathrm{obs.}}$ versus $[\mathrm{OH}^-]$ with positive slope and intercept (Fig. 4) indicates a deprotonation step prior to the transition state barrier and two competitive transition state steps (Rao et al., 1982, 1979). The rate of the intermediate formation may be given as:

$$\mathrm{Rate} = \frac{-\mathrm{d}[\mathrm{MnO}_4^-]}{\mathrm{d}t} = k_{\mathrm{obs.}}[\mathrm{MnO}_4^-] \qquad (1)$$

where

$$k_{\mathrm{obs.}} = (a + b[\mathrm{OH}^-])[\mathrm{MC}]_T \qquad (2)$$

Based on the advanced data, the following mechanism can be suggested

$$\mathrm{MC} + \mathrm{OH}^- \overset{K_1}{\rightleftarrows} \mathrm{MC}^- + \mathrm{H_2O} \qquad (3)$$

followed by the attack of permanganate in two competitive rate-determining steps as:

$$\mathrm{MC} + \mathrm{MnO}_4^- \overset{K_2}{\rightleftarrows} \mathrm{C}_1 \overset{k_a}{\rightarrow} [\mathrm{MC} - \mathrm{Mn}^{(\mathrm{VI})}\mathrm{O}_4^{2-}] \qquad (4)$$

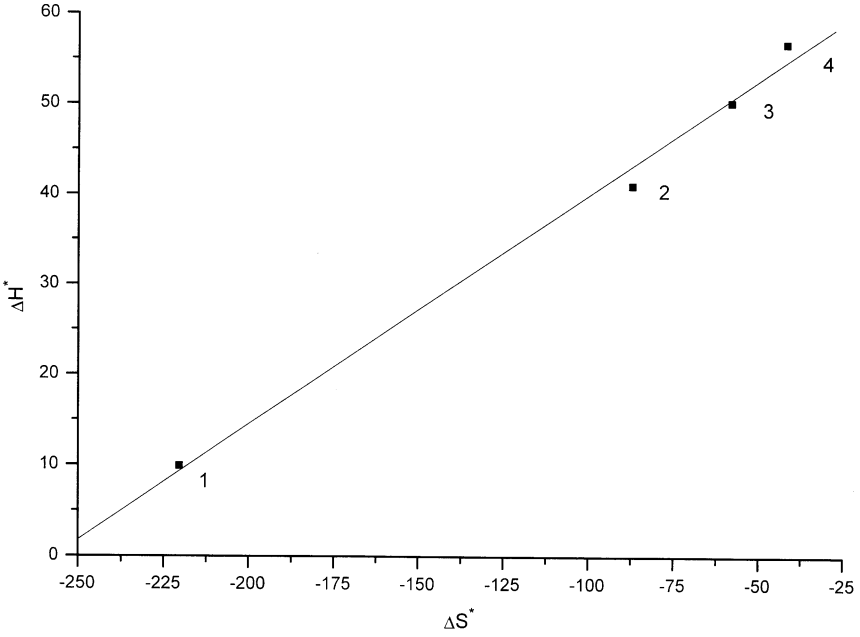

Fig. 10. Isokinetic plot ($\Delta H^{\#}$ versus $\Delta S^{\#}$) for the formation of the intermediate complex in the oxidation of polysaccharides by alkaline permanganate: (1) MC; (2) CMC; (3) sodium alginate; (4) poly(vinyl alcohol).

$$\mathrm{MC}^{-} + \mathrm{MnO}_4^{-} \overset{K_3}{\rightleftarrows} \mathrm{C}_2 \xrightarrow{k_b} [\mathrm{MC} - \mathrm{Mn}^{(\mathrm{VI})}\mathrm{O}_4^{2-}] \tag{5}$$

where K_1 is the dissociation constant of MC, K_2, and K_3 are the formation constants of the species C_1 and C_2, respectively, and k_a, k_b are rate constants of the rate-controlling steps for the formation of the $[\mathrm{MC{-}Mn^{(VI)}O_4^-}]$ intermediate complex via the decomposition of $C_1$and C_2. C_1 and C_2 involve metastable states of overlap of both Mn permanganate and oxygen alkoxide of MC molecular orbitals. Thus the oxidation of the polymers proceeds via one of two pathways, 4 or 5. Pathway 4 involves the attack of MnO_4^- on undissociated methyl cellulose (MC). But the second suggests the attack of MnO_4^- on the dissociated (MC^-) species (the enolate form). At any rate, the last step (5) may be the more intuitively favourable and reasonable pathway, particularly in the strong alkaline medium (pH ≥ 12) almost adjusted to carry out the investigated reaction.

On applying the steady-state approximation to the concentrations of intermediates C_1 and C_2 ($[C_1]_{\mathrm{ss}} = K_2[\mathrm{MC}][\mathrm{MnO}_4^-]$ and $[C_2]_{\mathrm{ss}} = K_3[\mathrm{MC}^-][\mathrm{MnO}_4^-] = K_1K_3[\mathrm{MC}][\mathrm{OH}^-][\mathrm{MnO}_4^-]$ one can derive the rate equation consistent with the proposed reaction scheme as follows:

$$\mathrm{Rate} = \frac{-\mathrm{d}[\mathrm{MnO}_4^-]}{\mathrm{d}t} = \frac{(k_aK_2 + k_bK_1K_3[\mathrm{OH}^-])[\mathrm{MC}]_T[\mathrm{MnO}_4^-]}{1 + K_1[\mathrm{OH}^-] + [\mathrm{MnO}_4^-](K^2 + K_1K_3[\mathrm{OH}^-]} \tag{6}$$

where $[\mathrm{MC}]_T = [\mathrm{MC}] + [\mathrm{MC}^-] + [C_1] + [C_2]$. Comparing Eqs. (1) and (6) under our experimental conditions used in this work, one may deduce that

$$k_{\mathrm{obs.}} = (k_aK_2 + k_bK_1K_3[\mathrm{OH}^-])[\mathrm{MC}]_T = k_2[\mathrm{MC}]_T; \quad \text{at constant } [\mathrm{OH}^-] \tag{7}$$

On matching Eq. (7) to the experimentally found Eq. (2), values for $a = k_aK_2 = 3.22$; $b = k_bK_1K_3 = 237$, could be determined, and from Eq. (7) it could be deduced that

$$K_{\mathrm{obs.}}^{-1} = \left(\frac{[\mathrm{OH}^-]}{2k_bK_1K_3} + \frac{1}{2k_aK_2}\right)\frac{1}{[\mathrm{MC}]_T} + k' \tag{8}$$

The validity of the suggested mechanism showed itself in many ways. The plot of $k_{\mathrm{obs.}}^{-1}$ against $[\mathrm{MC}]^{-1}$ (Fig. 3) at constant $[\mathrm{OH}^-]$ gave experimentally a straight line with a positive intercept (Michaelis & Menten, 1918) as the theoretical derived Eq. (8) demands. Moreover, the observed linear plot of [MC] $k_{\mathrm{obs.}}^{-1}$ versus $[\mathrm{OH}^-]^{-1}$ at constant [MC] (cf. Fig. 6) would present further convincing evidence of the reliability of Eq. (8) and hence of the foregoing mechanism. Furthermore, it is worth mentioning that further evidence that step 5 predominates over step 4 in the proposed mechanism arises from the relative values of *a* and *b* constants: ($b = k_bK_1K_3$ is almost 74 times greater than $a = k_aK_2$.

Again the effect of ionic strength indicates the catalytic salt effect and showed good agreement with the classical linear Debye–Hückel–Bronsted–Bjerrum–Livingston treatment of ln $k_{\mathrm{obs.}}$ versus $\sqrt{I}$ and $\sqrt{I}/(\sqrt{I} + 1)$ plots (cf. Figs. 7, 8) applied in the case of low ionic strengths

(Shaker, Alshehri & Burgess, 1998) and adopted here. This observed effect of the ionic strength on the reaction rate may further promote step 5 over step 4 in the assumed mechanism, in that the ionic species would be effective in the rate controlling step.

Furthermore, the activation parameters may provide some insight into the presented mechanism. The large negative value of $\Delta S^{\#}$ (cf. Table 1), would ascertain the inner-sphere electron transfer reaction and the formed compact intermediate complex (Hassan, 1993a,b; Hassan, Mousa & El-Shatoury, 1988a; Hassan et al., 1988b; Moore, 1962). On the other hand, the low value of activation energy (14.90 kJ mol^{-1}) indicates the ease of the reaction. Again, and as regards the positive $\Delta H^{\#}$ and $\Delta G^{\#}$ values, the endothermic formation of the intermediate and its non-spontaneity may be postulated (cf. Table 1). This evidence accords with the suggested transition state, i.e. the formation of the intermediate complex via the inner-sphere electron transfer scheme, when compared with those thermodynamic parameters determined for similar oxidation reactions of polysaccharides by permanganate (Hassan, 1993a,b; Hassan et al., 1988b).

The very low frequency factor in Table 1 (135 M^{-1} s^{-1}) may indicate the strictly compact formed intermediate complex (Moore, 1962). The activation parameters were computed, using Eyring Plot (Glasstone, Laidler & Erying, 1941), by least squares. Further evidence of the isokinetic oxidation of polysaccharides by alkaline permanganate has been confirmed by the observed good linear $\Delta H^{\#}$ versus $\Delta S^{\#}$ plot (Leffler & Grunwald, 1963), cf. Fig. 10. Hence, it can be concluded that the oxidation of polysaccharides, viz. sodium alginate, poly(vinyl alcohol) carboxymethyl cellulose, and methyl cellulose may follow the same scheme in alkaline permanganate oxidation. The value of $\Delta H^{\#}$ and $\Delta G^{\#}$ of the other three polymers were given from the literature (carboxymethyl cellulose is still submitted for publication).

At last and in accordance with the advanced documents on the catalytic salt effect, showing the ionic nature of the transition state, the base catalysed rate of the formation of the intermediate complex, indicating the pre-alkoxide formation equilibrium step, and the large negative entropy of activation, $\Delta S^{\#}$, revealing strictly compact formed complex accompanied by the observed low frequency factor; for all these reasons, the following identity of the [MC–Mn$^{(VI)}$O$_4^{2-}$] intermediate may be suggested:

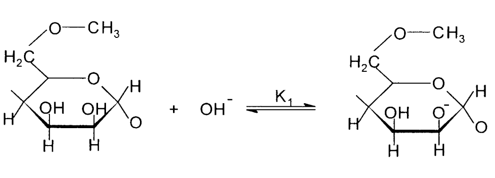

Methyl cellulose
[MC]

alkoxide

where K_1 represents the dissociation constant of MC

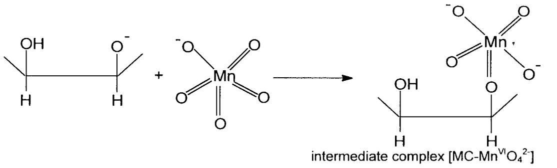

Hence, the intermediate is formed first by the attack of MnO_4^- ion on MC enolate (formed in the strong alkaline medium) and afforded the permanganate ester. Then one inner sphere electron transfer took place from MC alkoxide to MnO_4^- to the manganate ester as represented in Fig. 10 (Makhlouf et al., 1992; Sharpless, Teranishi & Backvall, 1955).

References

Carrington, A., & Symons, M. C. R. (1956). *Journal of Chemical Society*, 3373.

Glasstone, S., Laidler, K. J., & Eyring, H. (1941). *The theory of rate processes* (p. 417). New York: McGraw-Hill.

Hassan, R. M. (1993a). *Journal of Polymer Science, Part A: Polymer Chemistry*, *31*, 51–59.

Hassan, R. M. (1993b). *Polymer International*, *30*, 5–9.

Hassan, R. M., Abd-Alla, M. A., & El-Zohry, M. F. (1993). *Journal of Applied Polymer Science*, *47*, 1649–1652.

Hassan, R. M., Mousa, M. A., & El-Shatoury, S. A. (1988a). *Journal of Chemical Society, Dalton Transactions*, 601–603.

Hassan, R. M., Mousa, M. A., & Wahdan, M. H. (1988b). *Journal of Chemical Society, Dalton Transactions*, 605–609.

Jacky, M., & Simandy, L. I. (1972). *Journal of Chemical Society, Perkin Transactions*, *2*, 1481.

Jacky, M., & Simandy, L. I. (1976a). *Journal of American Chemical Society*, *98*, 1995.

Jacky, M., & Simandy, L. I. (1976b). *Journal of Chemical Society, Perkin Transactions*, *2*, 939.

Kumar, K., & Sakena, L. K. (1970). *Journal of Indian Chemical Society*, *47*, 435.

Leffler, L., & Grunwald, E. (1963). *Rates and equilibria of organic reactions* (p. 324). New York: Wiley (Also see p. 342).

Makhlouf, M. Th., El-Shatoury, S. A., & Hassan, R. M. (1992). *High Perfomance Polymer*, *4* (2).

Michaelis, L., & Menten, N. L. (1918). *Biochemie Z.*, *49*, 333.

Moore, W. J. (1962). *Physical chemistry*(3rd ed.). (p. 298). Englewood Cliffs: Prentice-Hall.

Rao, G. V., Rajanna, K. Ch., & Saiprakash, P. K. (1982). *Z. Physicalishe Chemie, Leipzig*, *263* (3S), 622–627.

Rao, V. S., Sethuram, B., & Rao, T. N. (1979). *International Journal of Chemical Kinetics*, *11*, 165.

Shaker, A. M., Alshehri, S., & Burgess, J. (1998). *Transition Metals Chemistry*, *23*.

Sharpless, K. B., Teranishi, A. Y., & Backvall, J. E. (1955). *Journal of American Chemical Society*, *78*, 1214.

Verma, R. S., Reddy, J. M. S., & Shastry, V. R. (1976). *Journal of Chemical Society, Perkin Transactions*, *2*, 469.

Wei, M. M., & Stewart, R. (1966). *Journal of American Chemical Society*, *88*, 1974.

Wiberg, K. B., & Geer, R. D. (1966). *Journal of American Chemical Society*, *88*, 5827.

Wiberg, K. W., Deutsch, C. J., & Rocek, J. (1973). *Journal of American Chemical Society*, *95*, 3034.